Article

AMERICAN ORTHOPAEDIC FOOT & ANKLE SOCIETY

Foot & Ankle Orthopaedics
2022, Vol. 7(3) 1–10

DOI: 10.1177/24730114221126457
journals.sagepub.com/home/fao

Displacement of the Metatarsal Sesamoids in Relation to First Metatarsophalangeal Joint Extension

Mackenzie French, MD[1,2], Eric D. Thorhauer, MS[2,3], Tadashi Kimura, MD, PhD[2,4,5], Bruce J. Sangeorzan, MD[2,4], and William R. Ledoux, PhD[2,3,4]

Abstract

Background: Quantifying normal sesamoid movement in relation to first metatarsophalangeal joint (MTPJ1) motion is essential to identifying aberrant kinematics and understanding how they may contribute to forefoot pain and dysfunction. The present study aims to report sesamoid displacement in relation to MTPJ1 extension and to compare sesamoid displacement with MTPJ1 range of motion (ROM) from several imaging modalities.

Methods: Using 10 fresh frozen cadaveric feet, sesamoid displacement was evaluated during simulated MTPJ1 extension. The ability of 3 MTPJ1 measurement techniques (goniometry, fluoroscopy, and unloaded cone beam computed tomography [CBCT]) in predicting sesamoid displacement were compared. Kinematics were expressed in a coordinate frame based on the specimen-specific first metatarsal anatomy, and descriptive statistics are reported.

Results: In the sagittal plane in both neutral and maximally extended positions, the tibial sesamoid was located on average more anteriorly than the fibular sesamoid. The angular displacement of the tibial and fibular sesamoids in the sagittal plane were 30.2 $\pm$ 14.3 degrees and 35.8 $\pm$ 10.6 degrees, respectively. In the transverse plane, both sesamoids trended toward the body midline from neutral to maximum extension. The intersesamoidal distance remained constant throughout ROM. Of the 3 measurement techniques, MTPJ1 ROM from CBCT correlated best ($R^2 = 0.62$ and 0.81 [$P < .05$] for the tibial and fibular sesamoid, respectively) with sagittal plane sesamoid ROM.

Conclusion: The sesamoids were displaced anteriorly and medially in relation to increasing MTPJ1 extension. CBCT was the most correlated clinical imaging technique in relating MTPJ1 extension with sesamoid displacement.

Clinical Significance: This study advances our understanding of the biomechanical function of the sesamoids, which is required for both MTPJ1 pathology interventions and implant design. These findings support the use of low-dose CBCT as the information gathered provides more accurate detail about bone position compared with other imaging methods.

Keywords: sesamoid, metatarsal extension, cone beam computed tomography, bone kinematics, metatarsophalangeal joint

Introduction

The anatomy of the tibial and fibular sesamoid bones is complex. They are 2 small bones of the first metatarsophalangeal joint (MTPJ1) housed within 2 grooves on the plantar surface of the metatarsal head.[2] The bones can be found embedded in the medial and lateral heads of the flexor hallucis brevis (FHB) tendon, which continues past the sesamoids to insert on the proximal phalanx at the tibial and fibular phalangeosesamoid ligaments.[20] The metatarsal crista protrudes from the plantar metatarsal head to separate the 2 grooves and is believed to assist in preventing subluxation of the sesamoids.[2,3] An association is maintained between the 2 sesamoids by the intersesamoid ligament (ISL), directly plantar to which the flexor hallucis longus (FHL) passes. There are no direct attachments between the sesamoids and the FHL. Insertions from the abductor and adductor hallucis tendons are also made on the tibial and fibular sesamoids.[10] The size of the medial

and lateral sesamoid bones are roughly 0.62 cm^2 and 0.82 cm^2, respectively.[8] A sufficient understanding of sesamoid anatomy is important to appreciate structures that are associated with their movement.

The sesamoids have a number of functions within the forefoot. They provide mechanical advantage to MTPJ1 through their position within the FHB tendon. Particularly in the push-off portion of gait, the sesamoids contribute to additional flexor strength by increasing the moment arm of the plantarflexors.[24] During normal gait, as much as 80% of bodyweight is transferred through the MTPJ1.[21] The sesamoids therefore also play an important role in both distributing weight from the force that the metatarsal would otherwise bear through its articulation on the metatarsal head[29] and offer protection to the FHL tendon that lies between the sesamoid grooves.[31]

The sesamoids are difficult bones to study using available imaging modalities because of their small size and location in a dense region at the MTPJ1. Current methods of observation include radiographs, ultrasonography, computed tomography (CT), and magnetic resonance imaging (MRI). Historically, clinical assessment has been from the tangential view of radiographs, which requires multiple images and extension of MTPJ1 to obtain an unobstructed sesamoid view.[1,17,32] Ultrasonograph presents similar difficulty with obstruction of view, but does have the benefit of showing real-time, dynamic motion of the bones. MRI and CT can both provide valuable 3D information but are associated with increased imaging times, costs, and radiation concerns for CT. It is also difficult to obtain physiological loading with MRI and CT scanners. However, low-dose cone beam CT (CBCT) scanning is becoming an increasingly available and standard clinical tool, alleviating some of the financial concerns while maintaining sensitive detectors with associated advanced reconstruction algorithms for more precise imaging at lower radiation doses to patients, all the while allowing for physiologic weightbearing.[15,18,33]

Because of their close association, it is important to understand the movement of the sesamoids in relation to MTPJ1 motion to gain a complete understanding of MTPJ1 and its associated pathology. It is known that sesamoid position has a connection with several forefoot pathologies.[7,13,23] A baseline analysis of normal displacement in relation to MTPJ1 motion is essential in understanding and identifying pathologic sesamoid movement. Regardless of imaging modality, if sesamoid displacement is observed, a clinician must know if that displacement is normal or not in order to include or exclude pathologic sesamoid displacement as part of a differential diagnosis.

The most detailed description of the sesamoids' positions in relation to MTPJ1 position is given by Jamal et al,[11] who found that in the sagittal plane they move anteriorly when MTPJ1 is extended from neutral. In the transverse plane through extension, the authors found a lateral excursion of both sesamoids. However, it is exceedingly difficult to quantify these data without considering the limitations in the testing procedures. Data in this study were acquired from the dissected MTPJ1s of embalmed cadavers and a coordinate measurement machine probe, which required a capsulotomy to access the sesamoids.

The primary aim of this study was to establish normative sesamoid displacement as it relates to simulated MTPJ1 extension. This was completed using high-resolution 3D scans of the sesamoids while maintaining the integrity and physiology of the MTPJ1. The secondary aim was to correlate the observed sesamoid displacement established in the primary aim with 3 clinical techniques of establishing MTPJ1 range of motion (ROM) including goniometry, fluoroscopy, and unloaded CBCT scanning. The information gained from this secondary aim may provide clinicians the ability to infer sesamoid displacement from information captured from MTPJ1 ROM for ease of diagnosing sesamoid pathologies in the future.

Materials and Methods

Ten fresh frozen cadaveric foot specimens (age: 45.0 ± 18.7 years; 4 female, 6 male; 2 paired, 6 unpaired) transected approximately 12 cm proximal to the ankle joint were obtained from accredited tissue banks (Innoved Institute, LLC, Elk Grove Village, IL and Lonetree Medical Donation, Centennial, CO). Specimens were thawed at room temperature overnight and screened for gross deformities, abnormal bony alignment at the MTPJ1, and bipartite sesamoids using preliminary fluoroscopy and CT scans. Normal foot alignments were confirmed by an orthopaedic surgeon by reviewing the imaging data (T.K.). Specimens were stored at –20 °C.

MTPJ1 ROM was determined via a goniometer. With the foot held in a standing position, an orthopaedic surgeon

[1]School of Medicine, University of Washington, Seattle, WA, USA
[2]RR&D Center for Limb Loss and MoBility (CLiMB), VA Puget Sound, Seattle, WA, USA
[3]Department of Mechanical Engineering, University of Washington, Seattle, WA, USA
[4]Department of Orthopaedics & Sports Medicine, University of Washington, Seattle, WA, USA
[5]Department of Orthopaedic Surgery, The Jikei University School of Medicine, Tokyo, Japan

Corresponding Author:
William R. Ledoux, PhD, RR&D Center for Limb Loss and MoBility (CLiMB), VA Puget Sound Health Care System, MS 151, 1660 S Columbian Way, Seattle, WA 98108, USA.
Email: wrledoux@uw.edu

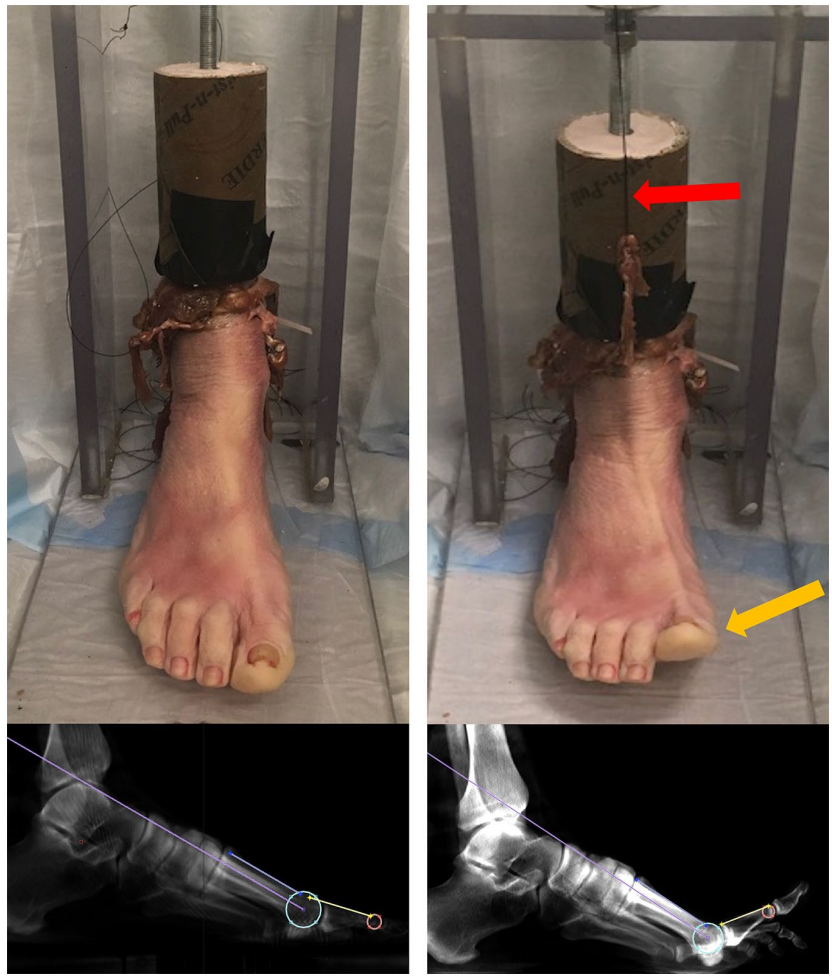

Figure 1. Specimen loaded in minimally attenuating plastic frame in CBCT scanner in neutral position and in maximum extension (yellow arrow) achieved through clamping a suture (red arrow) attached to the extensor hallucis longus. CBCT scan samples and the Shereff MTPJ1 angle measurement technique[14] are demonstrated from each pose. CBCT, cone beam computed tomography.

(T.K.) pushed superiorly on the plantar hallux until the natural limit of extension was encountered. The goniometer was centered at MTPJ1 and its arms aligned with the long axes of the first metatarsal and proximal phalanx. The angle of maximum extension was recorded as ROM, as is reported clinically.[35] Next, each foot was imaged with a Philips BV-Pulsera fluoroscope (12″ image intensifier, 0.293 mm/pixel) from a lateral view with the foot in neutral and the MTPJ1 in neutral and maximum extension. Force was directly applied to the extensor hallucis longus tendon to obtain the second position. A single rater (M.F.) made one angular measurement from the images using a custom-designed angle measurement tool in MATLAB (R2018a, MathWorks, Natick, MA). The standardized technique described by Shereff was implemented to obtain MTPJ1 angles from each image.[14] The neutral angle was subtracted from the maximum extension angle to calculate ROM.

Each of the 9 extrinsic ankle tendons were then dissected to approximately 3 cm above the ankle joint. Sutures were tied with a Krackow stitch (Ethilon No. 2 monofilament; Ethicon, Cornelia, GA) on the proximal end of the Achilles, extensor digitorum longus, extensor hallucis longus, peroneal longus, peroneal brevis, and tibialis posterior tendons, although only the extensor hallucis longus tendon was loaded in these experiments. The tibial and fibular shafts were denuded of tissues approximately 6 cm proximal to the ankle joint, and solid polyester resin cylinders were cast around the bones to provide a uniform interface to the biomechanical testing frame. The frame was assembled from acrylic and functioned to stabilize the specimen in a single pose through the duration of the scan. Metal that was used for clamping specimens into position was arranged far from the MTPJ1 to reduce X-ray scatter in the area of interest (Figure 1).

Each specimen was placed in the loading frame and was scanned in 3 configurations (neutral and maximum extension, plus an intermediate position) using a pedCAT CBCT scanner (voxel size = 0.3 mm isotropic; CurveBeam, Hatfield, PA). Neutral position was scanned and MPTJ1 angle was measured in MATLAB on a simulated lateral radiograph generated from the 3D CBCT data in CubeVue software (CubeVue, Hatfield, PA). This ensured a true lateral image that would be minimally affected by out-of-plane measurement errors. The MTPJ1 was then maximally extended by pulling on the extensor hallucis longus tendon, allowing the tendon to stretch to the natural limit of extension. The tendon suture line was clamped to maintain tension during the scan (Figure 1). MTPJ1 angles for maximum extension were measured in the same manner as in neutral position, and the neutral angle was subtracted from the maximum angle to calculate ROM from the CBCT. Specimens were returned to the freezer at –20 °C.

Specimens were thawed for a second time to determine the repeatability of the measurements. MTPJ1 angles from anonymized copies of 10 feet were remeasured using both the fluoroscopic and CBCT modalities, in both neutral and maximum extended positions. Measurements at both time points were repeated 3 times, and an intraclass correlation coefficient (ICC(A,1)) analysis was performed in order to quantify repeatability of the rater's measurement of MTPJ1 angles in the custom MATLAB software.

The sesamoids and first metatarsals were segmented from the CBCT scan volumes in Mimics (version 21, Materialise, Leuven, Belgium) in the neutral position. Bone kinematics between subsequent scans were determined via volumetric image registration in custom MATLAB software for each segmented bone (metatarsal, medial sesamoid, lateral sesamoid). Sesamoid kinematics were expressed as the position of each bone's center of mass in a coordinate frame based on the first metatarsal anatomy. This anatomy naturally lends itself to a cylindrical coordinate system with the capacity to account for metatarsal heads of varying sizes and shapes. A cylinder was fit to the manually selected distal metatarsal head's surface of articulation with the proximal phalanx (Figure 2). This cylinder defined an anatomical medial-lateral joint axis at the distal metatarsal. It was equally divided into a medial and lateral compartment as a simple means of normalizing size differences across specimens. In the sagittal plane, sesamoid position is expressed in the polar coordinate system centered at the medial-lateral axis. Using the circumference of the best-fit cylinder, 90 degrees was defined as the position parallel with the metatarsal diaphysis and 0 degrees was set orthogonal to this point in the plantar direction (Figure 3A). Sesamoid excursion in the transverse plane was reported as a percentage of their respective compartments' width, with 0% as the division down the diaphysis of the metatarsal (determined by the center of the medial-lateral division of the first cylinder) and 100% as the maximum width of the sesamoid's respective compartment (Figure 3B).

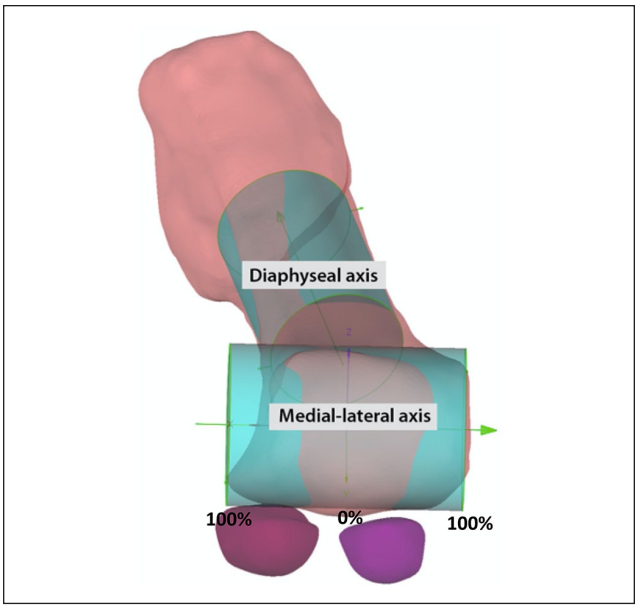

Figure 2. Cylinders were fit to each metatarsal head to create an anatomically based patient-specific coordinate system for sesamoid movement tracking.

All comparisons of means were descriptive in nature. Apparent ROM of the MTPJ1 in each modality was correlated with the sesamoid ROM in the sagittal plane using Pearson correlation coefficient (statistical significance $P < .05$).

Results

Our cadaveric testing rig produced physiological sesamoid bone movement that we were able to quantify with the CBCT and custom software. Displacement was observed in both sesamoids in all specimens. In the sagittal plane in a neutral position, the angle of the tibial sesamoid was greater on average than the fibular sesamoid, indicating that the tibial sesamoid rotated further anteriorly than the fibular (Table 1, Figure 3A). At maximum extension, the angle of the tibial sesamoid was again greater than that of the fibular sesamoid. From neutral to maximum extension, the ROM of the tibial and fibular sesamoids were 33.2 ± 10.7 degrees vs 35.8 ± 10.6 degrees, respectively. In the transverse plane, both sesamoids trended medially from neutral to maximum extension (Table 1, Figure 3B). The distance between the tibial and fibular sesamoids remained constant throughout ROM (Table 1, transverse excursion).

MTPJ1 angular measurements were consistent with intrarater scores of absolute agreements of ICC(A,1) = 0.95 for fluoroscopy and ICC(A,1) = 0.98 for CBCT. Comparison of ROM of MTPJ1 measured from 3 different modalities to

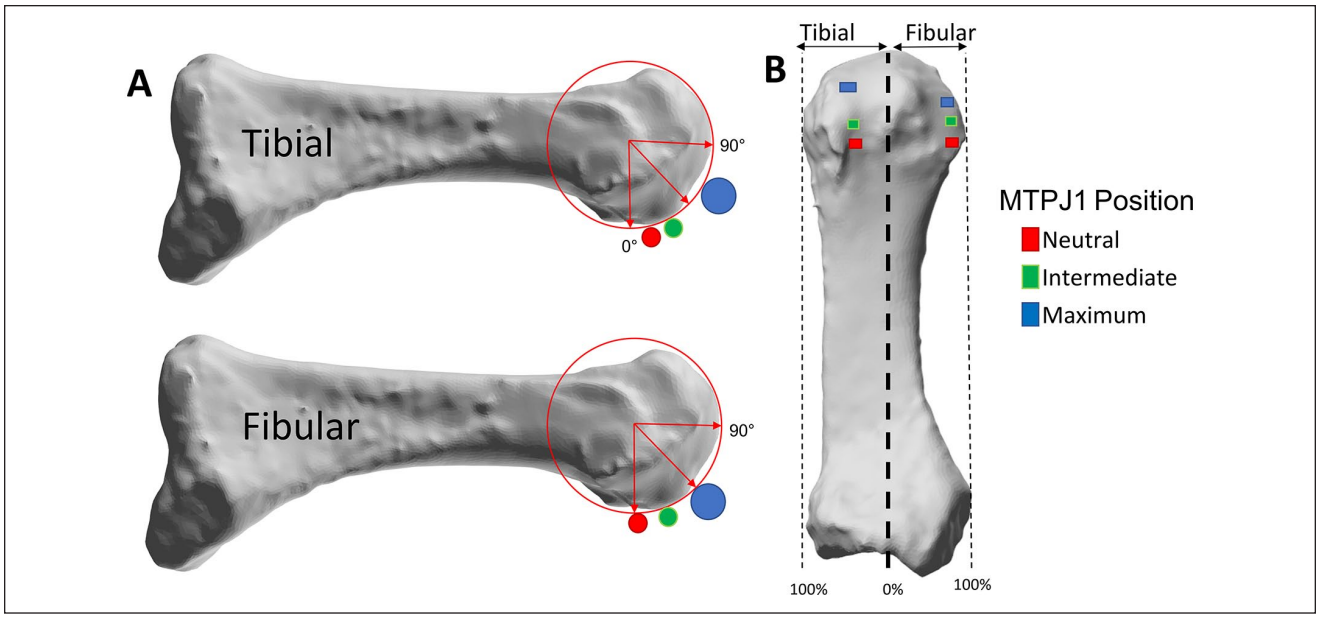

Figure 3. (A) Average tibial and fibular sesamoid position in sagittal plane (left foot, lateral view), defined as an angular position on a cylinder fit to the metatarsal head. The position parallel to the metatarsal diaphysis was defined as 90 degrees. In this plane, sesamoids rotated anteriorly on the head of the metatarsal with extension. (B) Cylinder fit over the metatarsal diaphysis was divided down the center (left foot, inferior view). The division was defined as 0% of the compartment, and the maximum compartment widths in the tibial and fibular directions were defined as 100%. Average sesamoid position in the transverse plane is reported as a percentage of its respective compartment. With extension, medial movement of both sesamoids is observed. Marker size demonstrates standard deviation.

Table 1. Sesamoid Position as a Function of MTPJ1 Flexion in Sagittal and Transverse Plane.

	SAGITTAL Angular Excursion		**TRANSVERSE** Excursion	
MTPJ1 Position	Tibial (degrees)	Fibular (degrees)	Tibial (%)	Fibular (%)
NEUTRAL	20.4 ± 5.4	5.3 ± 4.5	37.3 ± 14.2	80.0 ± 13.9
INTERMEDIATE	38.0 ± 5.7	22.7 ± 5.3	38.3 ± 12.8	77.0 ± 12.1
MAXIMUM EXTENSION	53.6 ± 5.4	41.1 ± 8.9	46.0 ± 18.7	69.8 ± 14.2

Abbreviation: MTPJ1, first metatarsophalangeal joint.

sagittal sesamoid ROM resulted in an R^2 of 0.13 and 0.05 with the goniometer, 0.13 and 0.29 in fluoroscopy, and 0.62 and 0.81 in CBCT for the tibial and fibular sesamoids, respectively (Figure 4); only the CBCT correlations were significant ($P < .05$). Descriptively, MTPJ1 ROM of each specimen obtained from the CBCT trials (range: 23.8-60.2 degrees, average 39.4 degrees) were greater than via fluoroscopy (range: 24.8-50.0 degrees, average 34.9 degrees) and both CBCT and fluoroscopy ROM differed from ROM calculated via goniometer (range 65-94 degrees, average 74.5 degrees).

Discussion

Through the use of an anatomically based, specimen-specific coordinate system, we successfully completed the primary (establish normative sesamoid displacement as it relates to simulated MTPJ1 extension) and secondary (correlate the observed sesamoid displacement established in the primary aim with 3 clinical techniques of establishing MTPJ1 ROM) aims of this study. Notably, we were able to use fresh frozen cadavers with unaltered MTPJ1s. This allowed us to gather data in a fashion most congruent with physiologic position, allowing for application to future clinical evaluation.

In the sagittal plane, we found the sesamoids rotate anteriorly around the natural cam shape of the distal metatarsal head. The tibial sesamoid was positioned at a greater angle on average than the fibular at both neutral and maximum extended positions. This suggests tibial sesamoid natural position is more distal on the metatarsal head than the fibular sesamoid. The total sagittal displacement of

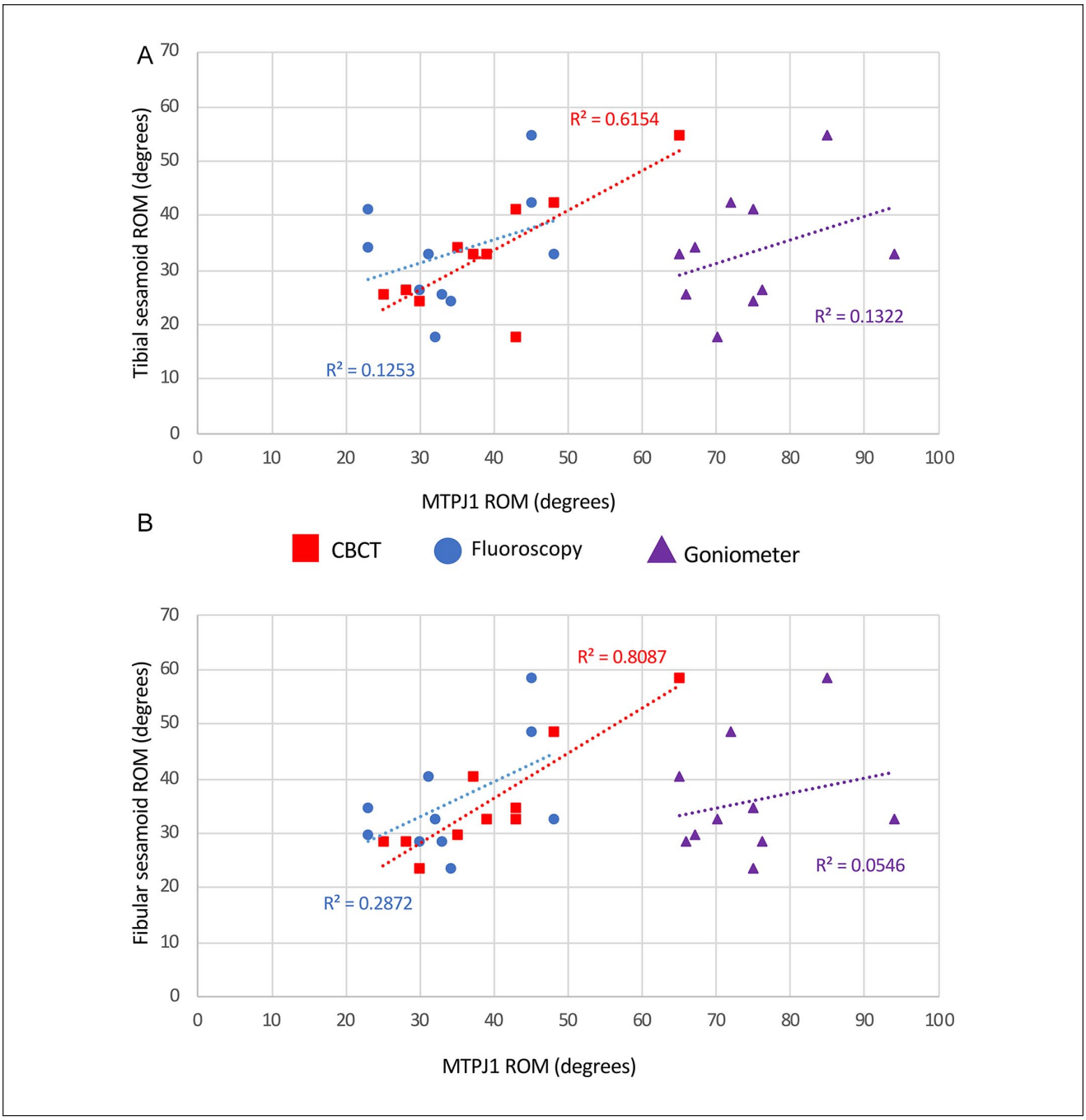

Figure 4. A comparison of the (A) tibial and (B) fibular sesamoid ROM with the ROM achieved from 3 different modalities: goniometer, fluoroscopy, and CBCT. Of the 3 imaging modalities, MTPJ1 ROM from CBCT was best correlated with sesamoid ROM. CBCT, cone beam computed tomography; MTPJ1, first metatarsophalangeal joint; ROM, range of motion.

each sesamoid was similar (Figure 3A). However, a previous paper reported a greater displacement of the tibial sesamoid than the fibular.[11] This difference in findings could be due to the embalming fluids or capsulotomies performed in the prior experiment, which may have altered the biomechanical integrity of the joint.

In the transverse plane, we found the distance between the sesamoids remained constant. Prior studies found that the fibular sesamoid had a greater overall excursion, suggesting that the sesamoids got further apart from one another in extension.[11] Again, methodologic differences could explain this, but without body weight loading in our

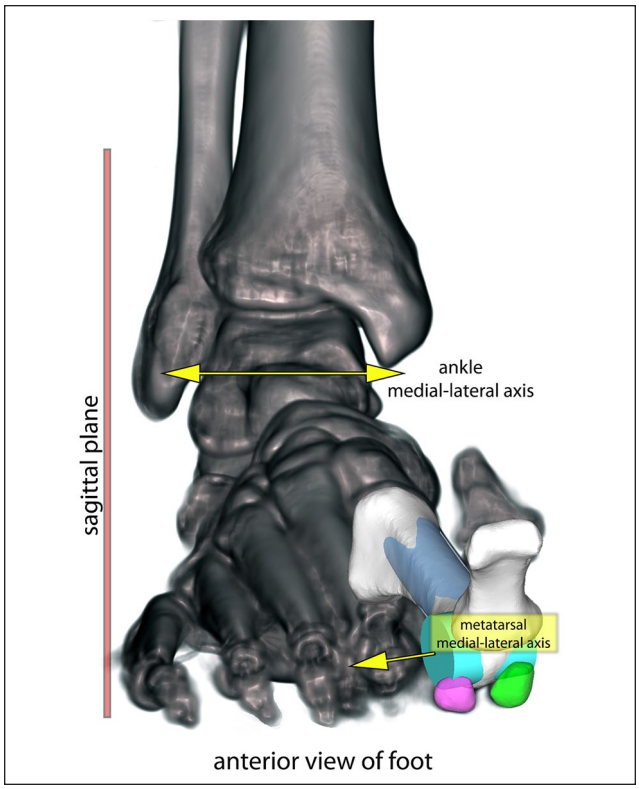

Figure 5. The medial-lateral axis of our coordinate system is defined based on a cylinder fit to the metatarsal head and is tilted in the coronal plane relative to ground. Furthermore, this axis is not normal to the foot sagittal plane defined by the ankle. With a tilted axis, as the sesamoids move anteriorly with extension, a component of their motion is captured as artificial medial displacement of the bones.

study, it is also possible that the ISL maintained fixed distance between the bones. There are reports of ruptured ISL that resulted in lateral displacement of the fibular sesamoid, and a resulting increased intersesamoid distance,[4,5] but our loading magnitudes and duration were too low to strain this ligament or induce viscoelastic creep, resulting in a near constant intersesamoid distance.

Although we observed medial displacement of the sesamoids with increasing MTPJ1 extension, we believe that limitations of our methods and coordinate system definitions may have confounded our results. Brenner et al[3] demonstrated that the crista is deviated on the longitudinal axis of the metatarsal head 7.99 degrees on average toward the lateral side of the metatarsal. With force applied and this bony boundary guiding the direction of the sesamoids, it is logical that the sesamoids follow this angle and move laterally. By fitting a cylinder to the head as part of our coordinate system, we created an artificial tilt in the coronal plane to the axis relative to the natural path of the sesamoids (Figure 5). With a tilted axis, as the sesamoids moved anteriorly with extension, a component of the motion was captured as artificial medial displacement of the bones. Additionally, rather than using the crista as a natural division, we created 2 artificial compartments to report medial-lateral sesamoid excursion by simply dividing the cylinder we fit to the head of the metatarsal in half (Figure 3B).

In relation to our secondary aim, we found that by using measurements from CBCT, we could best correlate sesamoid displacement with MTPJ1 extension. This correlation was stronger than that seen in the other 2 modalities of goniometry and fluoroscopy, which may support the transition to CBCT for studies of even the smallest bones in the foot and ankle. There has already been some use of CBCT in the evaluation of pathologic sesamoids,[13,16] but since its establishment, CBCT has been used mainly to examine the larger bones of the foot and ankle. Compared with radiographs, CBCT has shown to allow better visualization of the foot without inaccuracies in bone projection and better detection of correct bone angles.[25] CBCT should be considered in the future of clinical sesamoid evaluation.

One must consider the radiation exposure when choosing CBCT as the imaging modality for sesamoid visualization. Ludlow and Ivanovic concluded that effective dose for CT imaging is equivalent to just a few hours of background radiation, is negligible, and should not be considered in the decision to use CBCT.[19] Although planar radiographs involve even less dosage, they require multiple exposures to visualize the sesamoids, limiting that advantage. Ultrasonography, with no radiation dosage, has been shown capable of detecting symptomatic sesamoids,[28] and analyzing the position of the sesamoids in relation to pain in hallux valgus[38]; however, the more detailed and accurate information gained from the 3D CBCT images like complete bone morphology and assessments of bone quality should promote it to the optimal imaging technique, despite its higher radiation dosage.

This study was not without its limitations. First, as mentioned, in creating a coordinate system to report sesamoid location, a cylinder was fit to the shape of the metatarsal head. As a result, data are reported about the metatarsal head as the angular component of a polar sagittal coordinate. Although this better accounts for the eccentric orbit of the sesamoid about the cam-shaped metatarsal head in the sagittal plane, biological variation across specimens violates these geometric simplifications to some degree. Second, in comparing MTPJ1 ROM between different modalities, we used different methods of achieving maximum extension and used different calculations for ROM estimates. In the goniometric measurements, force was applied directly on the plantar great toe to generate extension. In the CBCT and fluoroscopic trials, maximum extension was obtained by pulling the extensor hallucis longus tendon at maximum resistance. Pulling on the tendon may have provided a mechanical advantage in the CBCT or fluoroscopic trials

that was not achieved in the goniometric trials. Third, the MTPJ1 ROM of the goniometric trials differs greatly from the other trials because the neutral position was not subtracted from maximum extension, making a direct comparison difficult but maintaining consistency with measurements and methods used clinically[35] (Figure 4). Fourth, other variability between the ROM measurement methods could be due to the poor reliability of goniometers[12,30,35,37] or inconsistent positioning of the ankle between trials. Fifth, in obtaining specimens for this study, some of the legs came paired, which may have confounded some results. Moreover, we did not explore the effect of sex in our analysis. Finally, we had to exclude 2 specimens because they contained bipartite sesamoids that would have made bone tracking difficult. As reports of congenital sesamoid absences are rare[6,9] and only occasional occurrences of bipartite sesamoids exist,[10] we feel that our results are still representative of the general population. Although our findings allow a general understanding of sesamoid kinematic through analysis of their displacement, these conditions are not entirely physiological as trials were unweighted. Future studies will use CBCT to examine sesamoid kinematics in weighted positions, simulating physiological forces exerted on the sesamoids, and biplane fluoroscopy for dynamic tracking of the sesamoid function during gait.

There are several aspects of this study that are of clinical significance. Generally speaking, to identify pathologic displacements of the sesamoids, it is essential to first understand normal displacement. This study provides that basis. From there, clinicians can begin to address how aberrant displacement of the sesamoids may contribute to forefoot pain and dysfunction. There are several well-known pathologies of the forefoot that may be associated with aberrant sesamoid displacement, but with limited analysis. Roddy and Menz reported that the MTPJ1 is the most common site of osteoarthritis (OA) in the foot.[26] Further, Van Saase et al and Wilder et al reported at least a 20% prevalence of OA at MTPJ1 in individuals older than 45 years.[34,36] Radiographic findings have shown that osteophyte formation and joint space narrowing is common in patients with MTPJ1 OA.[22] The failure of the sesamoids to rotate forward on the head of the metatarsal during the push-off portion of gait could leave the metatarsal head susceptible to injury. Knowledge of normal rotation as demonstrated here will allow clinicians to identify poor rotation in the future. The sesamoids are also involved in hallux valgus deformities, where they are shifted laterally relative to the metatarsal; however, this is a static finding, and dynamic sesamoid movement has not yet been studied in relation to hallux valgus development. The system we have developed for calculating sesamoid kinematics from CBCT scans has the capacity to detect small multiplanar movements, and in the future could be used to better quantify sesamoid position in hallux valgus patients and applied to diagnosing other pathologies.

The results of our study may help to inform the development of MTPJ1 implants that are sesamoid-preserving and further improve joint replacement outcomes. Schneider and colleagues showed that more anatomically minded MTPJ1 replacement designs resulted in better postreplacement MTPJ1 ROM in cadaveric specimens.[27] Advanced information on normal sesamoid tracking can allow for the development of novel implant designs to better represent normal anatomy at the MTPJ1 by including accurate sesamoid displacement. Further, extending these techniques to other pathologic populations, for example, hallux rigidus, might also provide insight into which patients should be fused, and which are candidates for a total joint replacement.

In conclusion, we reported sesamoid displacement in relation to MTPJ1 extension demonstrating anterior and medial sesamoid movement with increasing extension. Secondarily, we correlated sesamoid displacement with 3 clinical techniques of establishing MTPJ1 ROM and determined that CBCT was the most correlated technique to relate toe extension to sesamoid displacement. Quantitative data of the normal motion of sesamoids are necessary to understand how abnormal or diminished kinematics may contribute to forefoot pain, yet these data are scarce. As CBCT scanners become more common, we should strongly consider using them in the diagnosis of toe pathology relating to the sesamoids. These data will provide an accurate understanding of the normal displacement of the sesamoids and advance our understanding of their biomechanical function. It may later inform both interventions for MTPJ1 pathologies and implant designs.

Ethical Approval

Ethical approval was not sought for the present study because our institutions do not require it for cadaveric studies.

Declaration of Conflicting Interests

The author(s) declared no potential conflicts of interest with respect to the research, authorship, and/or publication of this article. ICMJE forms for all authors are available online.

Funding

The authors disclosed receipt of the following financial support for the research, authorship, and/or publication of this article: This work was supported in part by VA grants RX002357 and RX002970.

ORCID iD

William R. Ledoux, PhD, https://orcid.org/0000-0003-4982-7714

References

1. Alvarez R, Haddad RJ, Gould N. The simple bunion: anatomy at the metatarsophalangeal joint of the great toe. *Foot Ankle*. 1984;4(5):229–240. doi:10.1177/107110078400400502

2. Aseyo D, Nathan H. Hallux sesamoid bones. Anatomical observations with special reference to osteoarthritis and hallux valgus. *Int Orthop*. 1984;8(1):67–73. doi:10.1007/BF00267743
3. Brenner E. The intersesamoidal ridge of the first metatarsal bone: anatomical basics and clinical considerations. *Surg Radiol Anat*. 2003;25(2):127–131. doi:10.1007/s00276-003-0107-0
4. Capasso G, Maffulli N, Testa V. Rupture of the intersesmoid ligament of a soccer player's foot. *Foot Ankle*. 1990;10(6):337–339. doi:10.1177/107110079001000609
5. Crain JM, Phancao JP, Stidham K. MR imaging of turf toe. *Magn Reson Imaging Clin N Am*. 2008;16(1):93–103. doi:10.1016/j.mric.2008.02.002
6. Day F, Jones PC, Gilbert CL. Congenital absence of the tibial sesamoid. *J Am Podiatr Med Assoc*. 2002;92(3):153–154. doi:10.7547/87507315-92-3-153
7. Geng X, Zhang C, Ma X, et al. Lateral sesamoid position relative to the second metatarsal in feet with and without hallux valgus: a prospective study. *J Foot Ankle Surg*. 2016;55(1):136–139. doi:10.1053/j.jfas.2015.08.023
8. Ghimire I, Maharjan S, Pokharel GB, et al. Evaluation of occurrence of sesamoid bones in the lower extremity radiographs. *J Chitwan Med Coll*. 2017;7(2):11–14. doi:10.3126/jcmc.v7i2.22995
9. Inge GA. Congenital absence of the medial sesamoid of the great toe. *J Bone Jt Surg*. 1936;18(1):188–190.
10. Jahss MH. The sesamoids of the hallux. *Clin Orthop Relat Res*. 1981;157:88–97. doi:10.1097/00003086-198106000-00016
11. Jamal B, Pillai A, Fogg Q, et al. The metatarsosesamoid joint: an in vitro 3D quantitative assessment. *Foot Ankle Surg*. 2015;21(1):22–25. doi:10.1016/j.fas.2014.08.010
12. Janssen DM, Sanders AP, Guldemond NA, et al. A comparison of hallux valgus angles assessed with computerised plantar pressure measurements, clinical examination and radiography in patients with diabetes. *J Foot Ankle Res*. 2014;7(1):1–9. doi:10.1186/1757-1146-7-33
13. Katsui R, Samoto N, Taniguchi A, et al. Relationship between displacement and degenerative changes of the sesamoids in hallux valgus. *Foot Ankle Int*. 2016;37(12):1303–1309. doi:10.1177/1071100716661827
14. Kido M, Ikoma K, Ikeda R, et al. Reproducibility of radiographic methods for assessing longitudinal tarsal axes: Part 1: Consecutive case study. *Foot*. 2019;40:1–7. doi:10.1016/j.foot.2019.03.003
15. Kido M, Ikoma K, Imai K, et al. Load response of the medial longitudinal arch in patients with flatfoot deformity: in vivo 3D study. *Clin Biomech*. 2013;28(5):568–573. doi:10.1016/j.clinbiomech.2013.04.004
16. Kim Y, Kim JS, Young KW, et al. A new measure of tibial sesamoid position in hallux valgus in relation to the coronal rotation of the first metatarsal in CT scans. *Foot Ankle Int*. 2015;36(8):944–952. doi:10.1177/1071100715576994
17. Kuwano T, Nagamine R, Sakaki K, et al. New radiographic analysis of sesamoid rotation in hallux valgus: comparison with conventional evaluation methods. *Foot Ankle Int*. 2002;23(9):811–817. doi:10.1177/107110070202300907
18. Lintz F, Netto C de C, Barg A, et al. Weight-bearing cone beam CT scans in the foot and ankle. *EFORT Open Rev*. 2018;3(5):278–286. doi:10.1302/2058-5241.3.170066
19. Ludlow JB, Ivanovic M. Weightbearing CBCT, MDCT, and 2D imaging dosimetry of the foot and ankle. *Int J Diagnostic Imaging*. 2014;1(2):1. doi:10.5430/ijdi.v1n2p1
20. Marchetti DC, Chang A, Ferrari M, et al. Turf toe: 40 years later and still a problem. *Oper Tech Sports Med*. 2017;25(2):99–107. doi:10.1053/j.otsm.2017.03.001
21. McBride ID, Wyss UP, Cooke TDV, et al. First metatarsophalangeal joint reaction forces during high-heel gait. *Foot Ankle*. 1991;11(5):282–288. doi:10.1177/107110079101100505
22. Menz HB, Munteanu SE, Landorf KB, et al. Radiographic classification of osteoarthritis in commonly affected joints of the foot. *Osteoarthritis Cartilage*. 2007;15(11):1333–1338. doi:10.1016/j.joca.2007.05.007
23. Mortier JP, Bernard JL, Maestro M. Axial rotation of the first metatarsal head in a normal population and hallux valgus patients. *Orthop Traumatol Surg Res*. 2012;98(6):677-683. doi:10.1016/j.otsr.2012.05.005
24. Richardson EG. Injuries to the hallucal sesamoids in the athlete. *Foot Ankle Int*. 1987;7(4):229–244. doi:10.1177/107110078700700405
25. Richter M, Seidl B, Zech S, et al. PedCAT for 3D-imaging in standing position allows for more accurate bone position (angle) measurement than radiographs or CT. *Foot Ankle Surg*. 2014;20(3):201–207. doi:10.1016/j.fas.2014.04.004
26. Roddy E, Menz HB. Foot osteoarthritis: latest evidence and developments. *Ther Adv Musculoskelet Dis*. 2018;10(4):91–103. doi:10.1177/1759720X17753337
27. Schneider T, Dabirrahmani D, Gillies RM, et al. Biomechanical comparison of metatarsal head designs in first metatarsophalangeal joint arthroplasty. *Foot Ankle Int*. 2013;34(6):881–889. doi:10.1177/1071100713483096
28. Shin HY, Park SY, Kim HY, et al. Symptomatic hallucal interphalangeal sesamoid bones successfully treated with ultrasound-guided injection. *Korean J Pain*. 2013;26(2):173–176. doi:10.3344/kjp.2013.26.2.173
29. Sims AL, Kurup H V. Painful sesamoid of the great toe. *World J Orthop*. 2014;5(2):146–150. doi:10.5312/wjo.v5.i2.146
30. Somers DL, Hanson JA, Kedzierski CM, et al. The influence of experience on the reliability of goniometric and visual measurement of forefoot position. *J Orthop Sports Phys Ther*. 1997;25(3):192–202. doi:10.2519/jospt.1997.25.3.192
31. Srinivasan R. The hallucal-sesamoid complex: normal anatomy, imaging, and pathology. *Semin Musculoskelet Radiol*. 2016;20(2):224–232. doi:10.1055/s-0036-1581121
32. Talbot KD, Saltzman CL. Assessing sesamoid subluxation: how good is the AP radiograph? *Foot Ankle Int*. 1998;19(8):547–554. doi:10.1177/107110079801900808
33. Tuominen EKJ, Kankare J, Koskinen SK, et al. Weight-bearing CT imaging of the lower extremity. *Am J Roentgenol*. 2013;200(1):146–148. doi:10.2214/AJR.12.8481
34. Van Saase JLCM, Van Romunde LKJ, Cats A, et al. Epidemiology of osteoarthritis: Zoetermeer survey. Comparison of radiological osteoarthritis in a Dutch population with that in 10 other populations. *Ann Rheum Dis*. 1989;48(4):271–280. doi:10.1136/ard.48.4.271

35. Vulcano E, Tracey JA, Myerson MS. Accurate measurement of first metatarsophalangeal range of motion in patients with hallux rigidus. *Foot Ankle Int*. 2016;37(5):537–541. doi:10.1177/1071100715621508
36. Wilder F V., Barrett JP, Farina EJ. The association of radiographic foot osteoarthritis and radiographic osteoarthritis at other sites. *Osteoarthritis Cartilage*. 2005;13(3):211–215. doi:10.1016/j.joca.2004.10.021
37. Youdas JW, Bogard CL, Suman VJ. Reliability of goniometric measurements and visual estimates of ankle joint active range of motion obtained in a clinical setting. *Arch Phys Med Rehabil*. 1993;74(10):1113–1118. doi:10.1016/0003-9993(93)90071-H
38. Zeidan H, Ryo E, Suzuki Y, et al. Detailed analysis of the transverse arch of hallux valgus feet with and without pain using weightbearing ultrasound imaging and precise force sensors. *PLoS One*. 2020;15(1):1–17. doi:10.1371/journal.pone.0226914